Journal of Materials Chemistry A

Accepted Manuscript

This is an *Accepted Manuscript*, which has been through the RSC Publishing peer review process and has been accepted for publication.

Accepted Manuscripts are published online shortly after acceptance, which is prior to technical editing, formatting and proof reading. This free service from RSC Publishing allows authors to make their results available to the community, in citable form, before publication of the edited article. This *Accepted Manuscript* will be replaced by the edited and formatted *Advance Article* as soon as this is available.

To cite this manuscript please use its permanent Digital Object Identifier (DOI®), which is identical for all formats of publication.

More information about *Accepted Manuscripts* can be found in the **Information for Authors**.

Please note that technical editing may introduce minor changes to the text and/or graphics contained in the manuscript submitted by the author(s) which may alter content, and that the standard **Terms & Conditions** and the **ethical guidelines** that apply to the journal are still applicable. In no event shall the RSC be held responsible for any errors or omissions in these *Accepted Manuscript* manuscripts or any consequences arising from the use of any information contained in them.

RSC Publishing

www.rsc.org/materialsA

Registered Charity Number 207890

A Review on Hybrid Nanolaminate Materials Synthesized by Deposition Technique for Energy Storage Applications

Jalal Azadmanjiri[1], Christopher C Berndt[1,2], James Wang[1], Ajay Kapoor [1], Vijay K Srivastava[3], Cuie Wen[1,*]

[1] Faculty of Engineering and Industrial Sciences, Swinburne University of Technology, Hawthorn, Victoria 3122, Australia

[2] Department of Materials Science and Engineering, Stony Brook University, Stony Brook, NY 11794, USA

[3] Department of Mechanical Engineering, Indian Institute of Technology, BHU, Varanasi-221005, India

KEYWORDS: nanolaminates, magnetron sputtering, nanocomposites, dielectric materials, high permittivity

ABSTRACT: Nanostructured materials such as nanocomposites and nanolaminates are currently of intense interest in modern materials research. Nanolaminate materials are fully dense, ultra-fine grained solids that exhibit a high concentration of interface defects. They may be developed for engineering applications that take advantage of enhanced mechanical properties or for devices such as energy storage and memory storage capacitors. Nanolaminates can be grown using atom-by-atom deposition techniques that are designed with different stacking sequences and layer thicknesses. The properties of fabricated nanolaminates depend on their compositions and thicknesses. These can be demonstrated within the synthesis process by thickness control of each layer and interfacial chemical reaction between layers. In fact, dielectrics with the formed thin layer have efficient dielectric constant and high insulation characteristics. Dielectric materials of giant dielectric constants can be fabricated as modified single, binary and perovskite oxides.

A review of the advantages offered by nanolaminate structures for high performance energy storage devices is presented. Developments of dielectric materials that are formed from a thin layer approach are evaluated. The influence of the interface layer on the dielectric constant of nanolaminate films is assessed from the perspective in conferring a giant dielectric constant and high insulation characteristics. The incorporation of dopants and site-engineering techniques, as well as layer-by-layer structures; which can both be suitable for improving dielectric properties of dielectric nanolaminates, is detailed. Finally, the current status and development of artificial dielectric materials on high performance energy storage devices formed by dielectric nanolaminates is presented.

[*]Corresponding author. Tel.: +61 3 9214 5651; fax: +61 3 9214 5000.
E-mail address: cwen@swin.edu.au (Cuie Wen).

Journal of Materials Chemistry A Accepted Manuscript

Table of Contents

1 Introduction ………………………………………………………………………. 3
1.1 Dielectric materials: structures, compositions, properties and applications ……..... 4
1.2 Nanolaminate materials ………………………………………………………….... 5
1.3 Synthesis of nanolaminates by deposition methods ……………………………….. 6
2 Dielectric nanolaminate materials for energy storage ………………………………. 8
2.1 Sublayer thickness and interface layer effect on electrical characteristics …………. 9
2.2 Effect of doped materials on electrical properties of dielectric nanolaminates ……. 10
2.3 Effect of layer-by-layer structure on dielectric breakdown strength ………………. 11
3 Nanolaminates properties for high performance energy storage devices ………….. 12
3.1 Electrical characterization and dielectric properties of metal oxide nanolaminates ... 13
3.2 Al_2O_3 nanolaminate structure and post-deposition annealing effects ……………… 14
3.3 Novel mixed metal phosphonate nanolaminates for high dielectric composite materials ……………………………………………………………………….. 16
3.4 Development on artificial ferroelectric nanolaminates for energy storage devices … 17
4 Summary ………………………………………………………………………. 18
5 Acknowledgments ……………………………………………………………….... 18
6 References ……………………………………………………………………….... 18

Journal of Materials Chemistry A Accepted Manuscript

1. Introduction

Two dimensional nanosheets are considerable interest, especially in new compound materials with high permittivity for electronic applications such as high efficiency energy storage devices. The synthesis of one and three dimensional nanomaterials has been well documented. In contrast, two dimensional nanomaterials have been less comprehensively studied due to their distinctive synthetic process [1]. On the other hand, fundamental research has been increasingly focused on inorganic nanosheets because of their potential in insulators, semiconductors and conductors. The applications of inorganic nanosheets depend on their chemical composition and atom arrangements [1]. Furthermore, most inorganic nanosheets are electrically insulated or exhibit a wide semiconducting band gap [2, 3], as well as having high chemical and thermal stabilities [1].

Metal oxides, such as HfO_2, TiO_2, Ta_2O_5 and ZrO_2, have been considered for high dielectric constant materials with high permittivity value [4, 5]. Note that the dielectric constant is denoted as κ, and is also referred to as the relative permittivity (ε_r). The dielectric constant is defined as the ratio of the permittivity of the dielectric (ε) to the permittivity of a vacuum (ε_o). However, the metal oxides have a narrow band gap with a large leakage current [4, 6]. In addition, most high dielectric constant materials are thermodynamically unstable when in contact with a silicon wafer at high temperatures [4, 7]. The thermal stability and leakage current of some metal oxides have been improved using an additive that exhibits good thermal stability and a large band gap [8-12]. However, the dielectric constants of some composites are reduced due to the relatively low dielectric constant of the additive [11]. Hence, development of integrated devices with new composite materials that can demonstrate good insulating and high permittivity values has become a critical issue for microelectronic materials.

The design and fabrication of hybrid dielectric materials with high permittivity (high-ε), high stability and low leakage current are being investigated using vapor deposition methods. The synthesis of high performance dielectric materials by investigating hybrid nanolaminates containing different layers is being pursued. Usually, nanolaminates are composite films consisting of alternating layers of different materials with nanometer scale thickness. Nanolaminates are fully dense and ultra-fine grained with high concentration of interface defects. The manufacturing process of nanolaminates via vapor deposition routes typically produces highly textured layers with close packed lattice planes of the layer materials in the plane of the multilayer [13].

Magnetron sputtering is a physical vapor deposition process that can be employed to manufacture multilayered materials. In such sputter deposition systems, the atoms are formed in the vapor phase by bombardment of a solid source material with energetic particles. In this fashion, a single layer of material is deposited onto the substrate; which is normally a silicon wafer. The current work uses

Journal of Materials Chemistry A Accepted Manuscript

the magnetron sputtering method repetitively to manufacture disparate layers. The microstructure and properties of the nanolaminates depend on their composition. The thickness can be controlled within synthesis by control of the thickness of each layer and interfacial chemical reaction between the two layers. The structure and composition also can be manipulated by changing the processing parameters.

In this article, we present a review of hybrid high permittivity dielectric nanolaminates synthesized by atomic layer deposition is presented. The technological use of these materials is aimed towards the electrical materials field of high efficiency energy storage devices.

1.1 Dielectric materials: structures, compositions, properties and applications

A dielectric material is an electrical insulator that can be in the form of a solid, liquid or gas. Dielectrics exhibit dipole structures where the dipoles will generally be in random orientations unless an electric field is applied. When a voltage is applied to a dielectric, the dipoles rotate and align themselves in the field so that electrical polarization occurs. Figure 1 illustrates the polarization of a dielectric in an external electric field. The positive charges in a dipole are displaced minutely in the direction of lower voltage and the negative charges in dipoles are displaced minutely in the opposite direction. Polarization in a dielectric decreases the effective electric field between the plates and increases the capacitance of the parallel plate structure.

Figure 1

A dielectric material is characterized by relative permittivity, ε_r, or dielectric constant κ; which is an intrinsic material property. The relative permittivity demonstrates the ease of the polarization of the material and determines the size of the surface charge densities on both sides of a dielectric. A key challenge in microelectronics research is the synthesis of high permittivity dielectrics with low dimension size for microelectronic devices such as memory [14-18], capacitors [19, 20], gate insulators [16, 21-23], energy storage [24, 25], and high frequency applications in communication devices [1, 26]. Therefore, dielectrics require higher permittivity (ε_r), lower loss tangent (tanδ) and reduced leakage current (J) [1]. Thus, capacitors with a giant dielectric permittivity are under investigation [1] with the potential that these dielectrics replace SiO_2 at gate insulators in silicon devices due to the relatively low permittivity of SiO_2 (ε_r= 3.9) [16, 21, 22].

These materials can be divided into two categories on the basis of the polarization nature of dielectrics. One group is based on metal oxides such as Al_2O_3 [21, 27], TiO_2 [21, 28, 29], Nb_2O_5 [27, 30], HfO_2 [21], ZrO_2 [21], and Ta_2O_5 [21, 27], with nonpolar atomic arrangements [1]. In this

Journal of Materials Chemistry A Accepted Manuscript

group of dielectrics the residual polarization can remain long after the applied voltage is removed [31]. This phenomenon is called dielectric relaxation [31]. Metal oxide dielectrics have low loss (tan δ) and a relatively low temperature coefficient (τ). However, the relative permittivity (ε_r) of this group is typically less than 100 [1].

Another group of dielectric materials is ferroelectrics with residual dipoles resulting from static atomic displacements that display principally, perovskite structures [1]. The relative permittivity (ε_r) of this group of dielectric materials is more than 200 [1]. However, the dielectric constant of perovskites, including ferroelectric oxides ($Pb(Zr,Ti)O_3$) and relaxor oxides ($PbMg_{1/3}Nb_{2/3}O_3$), has been improved to above 1,000 [16, 20, 21]. The dielectric constant of the two perovskites varies with temperature, so that it is inconvenient for some applications such as capacitors [1]. Some applications require a static and stable dielectric constant with respect to temperatures to avoid device failure. Table 1 shows a list of current dielectric materials with different compositions and high dielectric constant.

Table 1

Contemporary research is focused on nanolaminates and phase mixtures such as TiO_2-Ta_2O_5 [29], TiO_2-Nb_2O_5 [30], Nb_2O_5-Ta_2O_5 [27-31, 34] and ZrO_2-Ta_2O_5 [35] with the aim of creating a device that exhibits a highly stable dielectric constant (κ) with a low loss tangent (tanδ). Recently several dielectric compounds with a giant dielectric constant, such as $CaCu_3Ti_4O_{12}$ ($\varepsilon_r > 80,000$), have been reported [36]. However, thin films of these giant components exhibit dielectric constants that are several magnitudes less than bulk values [1]. Hence, designing and manufacturing thin film materials with high-κ characteristics is a challenge for the technological areas of nanoelectronics and energy storage.

1.2. Nanolaminate materials

A nanolaminate is a thin film created from multiple layers of two or more materials with layer thicknesses of one hundred nanometers or less. Nanolaminates with thin film structures have high interfacial density that demonstrates significantly different properties than their bulk constituents. Figure 2 shows an example of a nanolaminate consisted of alternating Al_2O_3/ZnO layers fabricated by atomic layer deposition (ALD). The electrical and structural properties of Al_2O_3/ZnO nanolaminates [37, 38] can be tuned over a wide range, whereas the bulk Al_2O_3 or ZnO components do not exhibit insulator and conductor properties that are the same as these nanolaminates.

Journal of Materials Chemistry A Accepted Manuscript

The inference from the viewpoint of processing is that the microstructure and properties of nanolaminates can be tuned during synthesis by thickness control of each layer and interfacial chemical reactions between each layer. Hence, extensive investigation is being undertaken to develop nanolaminates with unique and highly specific physical, mechanical and chemical properties. These novel properties generally occur when the synthesized nanolayer thicknesses are less than the length scale that defines the physical property [39]. For instance, the hardness of a nanolaminate film will be increased when the nanolayer thickness is less than the slip plane dislocation distance [40, 41]. Low thermal conductivity nanolaminates also arise when the thicknesses of layers are less than the phonon mean free path [42, 43].

Nanolaminates manufactured from ultra-thin films can represent a new platform for engineering by replacing traditional materials. They can also open up opportunities for new technological applications due to their nanometer scale structures and thicknesses [44]. Optimization and development of dielectric nanolaminates for various applications such as memory storage capacitors [45], charge storage [46, 47] and altering the voltage coefficient of capacitance [48] is an emerging topical area. Additionally; composition, thickness and laminate structure are essential design factors for nanolaminates [49-53] and these can be obtained by suitable advanced processing techniques. Therefore, physical and chemical vapor deposition methods have been implemented to synthesize thin film layers for nanolaminates.

Figure 2

1.3. Synthesis of nanolaminates by deposition methods

Nanolaminates are nanocomposites that can be fabricated by several deposition techniques. This processing method can be used to produce thin films and multiple layers in the nanometer range with appropriate conformity and process control [54-56]. There are two categories depending on whether the process is chemical or physical [57]. The chemical and physical methods are further differentiated of the basis of phase of the precursor [58].

Atomic layer deposition (ALD) or atomic layer epitaxy (ALE) is a chemical deposition method for producing high-quality, large-area surface and thin film layers with atomic scale precision [54]. Figure 3 presents a schematic illustration of an ALD [55, 56] method where the thin film layers cyclically grow for a binary compound from gaseous precursors. ALD is a surface controlled layer-by-layer thin film deposition process. It has the greatest potential for producing thin films with control of the thickness and composition of the films at the atomic level. It can produce a wide range of film materials with high density, low impurity and accurate control of thickness. As well, a

Journal of Materials Chemistry A Accepted Manuscript

low deposition temperature can militate against adverse effects on sensitive substrates. ALD has been successfully applied for deposition of oxide materials such as high dielectric constant insulators [59, 60].

Figure 3

The ALD method has been widely considered by researchers in nanotechnology areas due to its control over the deposited layer thickness of materials and the potential for modification of chemical and physical properties in the nanoscale range [54]. There is a comprehensive review on metal and nitride thin films fabricated by ALD for semiconductor device applications by Kim [61]. The surface chemistry of the trimethylaluminum/water process by ALD is elaborated by Puurunen [62]. Moreover, HfO_2 is considered for electronic applications [63], and the electrical and mechanical properties of some metal oxides such as ZnO [64], TiO_2 [65] and Al_2O_3 [66] have been investigated systematically [54]. Other groups have developed deposition processes for metals such as platinum and ruthenium for electrode material applications [62]. Slowness of deposition is the major limitation of the ALD technique. However, this issue is somewhat ameliorated due to the rapid growth of the thin layer device.

Sputtering was first used in the laboratory to either (i) enable anodic deposition of a material from a gaseous discharge, or (ii) to remove a material from a surface under a reversed electrode polarity [67]. Generally, sputtering takes place in a chamber filled with a gas such as argon. The target, or source material, is located on one side of the chamber while the substrate onto which the deposit will form is placed on the opposed side. A high direct current (DC) voltage is applied between the target and the walls of the chamber. Alternating current (AC) voltage can also be used when the target materials are insulators. The applied voltage will ionize the gas into a plasma, with the voltage drop occurring in a thin region, called the dark space sheath, close to the target. When a gas ion enters the dark space sheath, it will be strongly accelerated by the voltage drop, and hit the target violently so as to displace atoms, molecules or clusters of atoms from the substrate. The pressure in the chamber is maintained at a low level so that the mean free path is greater than the physical size of the chamber. Hence, most of the separated particles from the target collide against the substrate without losing their high energy in secondary collisions. Therefore, a thin layer of the target material will be created on the substrate.

Sputtering by this method onto the substrate is slow, which may cause overheating and structural damage because of unwanted bombardment by electrons from the plasma. Consequently, magnetron sputtering was developed to resolve these issues.

Journal of Materials Chemistry A Accepted Manuscript

Electrons in the chamber can be trapped by a magnetic field, such as in a magnetron sputtering device. The magnetic field can be created by a permanent magnet or electromagnet, or a combination of both [68]. Thus, atoms in a magnetron sputtering discharge are sputtered from the cathode target by a magnetically confined plasma. The target material is sputtered by the bombardment of high energy ions accelerated over the cathode sheath potential. Secondary electrons are emitted and accelerated away from the target surface as a result of the ion bombardment. A magnetic field confines the ionizing energetic electrons near the cathode, thereby allowing operation at high plasma densities and low pressures. Figure 4(a) shows a two dimensional nanosheet with atomic or molecular thickness that can be produced by the magnetron sputtering technique. Figure 4(b) shows a schematic diagram for the synthesis of a thin film deposited onto a silicon substrate *via* magnetron sputtering.

Figure 4

Magnetron sputtering can produce high quality, low impurity films at rapid deposition rates. This has become the process of choice for the deposition of a wide range of functional coatings. In addition, magnetron sputtering has the advantages of good control of the coating composition, thickness, good adhesion between the layers and a low substrate temperature during deposition [69].

Hence, nanolaminates can be fabricated by magnetron sputtering. Magnetron sputtering has been applied to the deposition of oxide materials with a high dielectric constant onto metal sheets and other ultrathin metal oxide films for electronic device applications [49, 70, 71]. Figure 5 depicts a multilayered organic electronic device and metal oxide buffer layers. Greiner et al. [70] synthesized metal films (MoO_3 nanoplates) of 200 nm thickness using 99.99% pure metal targets *via* magnetron sputtering.

Figure 5

2. Dielectric nanolaminate materials for energy storage

Dielectric materials with a high dielectric constant play critical roles in a wide range of electronic applications and they can be used in high efficiency energy storage devices [49]. With the fast growth of micro and nano electronic devices, high performance dielectric materials are required with high dielectric strength, high dielectric permittivity, low dielectric loss, and high tunability in a wide frequency range [72-75]. Studies have concentrated on developing the current existing dielectrics and investigating new high dielectric constant materials. Dielectric materials can be

Journal of Materials Chemistry A Accepted Manuscript

single oxide such as Ti oxides [76, 77, 78], Ta oxides [79], Hf oxides [80] and Mn oxides [81]; binary oxides such as $Ti_xAl_{1-x}O_y$ [82], $Hf_xAl_{1-x}O_y$ [83]; and perovskite oxides such as $BaTiO_3$ [84] and $SrTiO_3$ [85].

Dielectric nanosheets are able to achieve a giant dielectric constant and high insulation characteristics due to the formed thin layers. These parameters are essential for high performance capacitors. One significant achievement has involved developing dielectric nanolaminates with unique physical and chemical properties. Li et al. [49] indicated that modifying composition at interfaces in nanolaminate structures, including layers of two different materials (AlO_x, TiO_y) with low dielectric constant, can contribute to dielectric polarization under an externally applied field and, hence, enhance the dielectric constant of the layered structures, Figure 6. The enhanced dielectric constant may be attributed to the internal barrier layer capacitors due to the presence of electrical inhomogeneity in the thin film materials [49, 86]. This result indicates that the dielectric properties of materials can be altered significantly by employing the design concept of nanolaminate structures.

Figure 6

2.1. Sublayer thickness and interface layer effect on electrical characteristics

Park et al. [87] reported on a nanolaminate of Al_2O_3 and HfO_2 sublayers that was deposited using plasma-enhanced atomic layer deposition. The nature of the interface was affected by the thickness of the sublayers and revealed a significant influence on the dielectric constant of the nanolaminate. Thus, the physical properties of nanolaminate structures can be adjusted by adjusting the composition and the thickness of the binary oxide sublayers. Nanolaminates with unique electrical, mechanical, magnetic and thermal properties can be achieved by designing the composition and thickness of sublayers. These properties and characteristics cannot be obtained in bulk films that exhibit a larger scale of thickness [87-91]. For instance, the dielectric constant of the nanolaminate was influenced by the sublayer thickness in the HfO_2/Al_2O_3 nanomixture and nanolaminate films before and after annealing, as shown in Figure 7.

Figure 7

The dielectric constant increased rapidly [87] when the sublayer thickness decreased from 30 to 10 Å. This rapid increase in the dielectric constant arose due to the precipitation of an interfacial

Journal of Materials Chemistry A Accepted Manuscript

layer of Hf-O-Al between two different sublayers during annealing and the number of interfaces between the two sublayers increased radically when the sublayer thickness decreased.

Patscheider et al. [92] investigated the electronic structure of the SiN_x/TiN interface and indicated that the high concentration of nitrogen in Si_3N_4 gave rise to interface polarization due to the formation of an interlayer. The high nitrogen concentration enhanced polarization and strengthened interfacial bonding. The effect of interface interactions in nanolaminates and their technological applications have been investigated extensively [70, 87, 92-94].

2.2. Effect of doped materials on electrical properties of dielectric nanolaminates

The dielectric performance of a nanolaminate is related to its structural features. The incorporation of dopants and site-engineering techniques are alternative methods to improve the electrical properties and permittivity of dielectric nanolaminates that exhibit ultrathin layers of known high permittivity and low leakage oxide [27, 95-97]. Chaudhuri et al. [95] suggested that nitrogen consolidation in hafnium based dielectrics could moderate the leakage current. In other studies [98-100], it was demonstrated that significant improvement of the electrical properties can be observed for HfO_2 thin films doped with fluorine, nitrogen or lanthanum. Likewise, it was found that carbon doping in different oxides can improve the dielectric properties and reduce leakage current densities of Ta_2O_5 films [101].

Osada et al. [1] reported that A-site modification in perovskite layers, for instance $SrBi_2Ta_2O_9$ and $Bi_4Ti_3O_{12}$, has been proposed to tilt the TiO_6/TaO_6 octahedral and enhanced the dielectric and ferroelectric properties. Additionally, they declared that B-site substitution with higher valence ions improved the leakage and fatigue properties by reducing oxygen vacancies [1]. Figure 8 shows how A- and B-site modifications with Sr^{2+} ions in $Ca_2(Nb/Ta)_3O_{10}$ nanolaminates can improve the dielectric constant and leakage current density. The replaced Sr^{2+} ions in the A-site improved the dielectric constant value, while the B-site conversion with Ta^{5+} ions increased the leakage current characteristics and decreased the permittivity value.

Figure 8

As well as these examples of site engineering, extensive investigations into complementary metal oxide semiconductor devices have been performed to increase the charge storage capability of the dielectric. Some binary or mixtures of metal oxides, such as ZrO2, Ta2O5, Nb2O5, TiO2 or Al2O3, have been considered to replace SiO_2 [27, 52, 56]. Among these binary compounds, TiO_2 exhibits the highest dielectric constant, but the band gap for this metal oxide is low [52]. On the other hand,

Journal of Materials Chemistry A Accepted Manuscript

Al_2O_3 shows the highest band gap and resistance, but the relative dielectric constant of Al_2O_3 is low [27]. Jõgi et al. [52] showed that $Al_xTi_yO_z$ mixtures and Al_2O_3-TiO_2-Al_2O_3 nanolaminates were composites with high dielectric constants that can be used in electronic devices. Although the thin film layers of Al_2O_3-TiO_2-Al_2O_3 were revealed to have good capacitive properties, the leakage current density of this mixture was not as good as pure Al_2O_3 [102, 103]. Table 2 lists some synthesized mixture nanolaminate systems with notable performance parameters.

The work on dielectric nanolaminates can provide a new formulation for designing functional high dielectric constant devices. The use of doping to manipulate dielectric properties is a well-known technique in traditional bulk dielectrics. This technique is useful in tailoring the dielectric properties of individual nanolaminates. The method also creates new possibilities for systematically tuning the performance of high dielectric constant oxides in miniaturized electronic component [1].

Table 2

2.3. Effect of layer-by-layer structure on dielectric breakdown strength

Dielectric materials with high potential dielectric strength (E_{BD}) combined with high dielectric permittivity (ε_r) are significant for advanced power systems that challenge both high energy and power densities, such as pulsed power capacitors [112]. The dielectric strength is the maximum electric field strength that can be tolerated without break down and failure of insulating properties. Here, the advanced power devices are suitable for future high power density automotive and aerospace technologies.

The high performance devices need to have a storage energy system in the form of dielectrics with a high energy density, great maximum voltage limit, and scalable uniform defect free film construction [112, 113]. Nanocomposite structures are being considered for this application [114, 115]. For instance, Kim et al. [116] reported that by incorporation 50 vol% $BaTiO_3$ in P(VDF-HFP) polymer the relative permittivity can be increased to 32 and the theoretical energy density is 15-20% (up to 5.6 J/cm^3) more than unfilled P(VDF-HFP). In another study, Li et al. [117] indicated a relative permittivity improvement to 54 and an energy density of 6.9 J/cm^3 by incorporating 30 vol% $BaTiO_3$ nanoparticles as a filler into P(VDF-TrFE-CTFE) polymer. However, these nanocomposite structures can also provide facile pathways for carrier migration [112], therefore, leading to increased conduction loss and lower breakdown field strength than the pure matrix; thus compromising the attainment of the highest energy storage.

Technologies arising from theoretical and experimental investigations showed that a tailored architecture manufactured by controlling the layer-by-layer assembly of functional nanosheets *via*

Journal of Materials Chemistry A Accepted Manuscript

advanced physical or chemical methods can improve the high field response with high dielectric permittivity [1, 113]. Dielectric nanosheets with a high dielectric constant were combined with various materials such as single nanolayers or different compositions, Figure 9. Fillery et al. [112] fabricated a modified organic system of montmorillonite (oMMT) and polyvinyl butryal (PVB, $(C_8H_{14}O_2)_n$). The synthesized uniform films demonstrated that the E_{BD} of the nanolaminates increased 2.5 times in comparison to the unfilled polymer.

This improvement in breakdown strength for the nanolaminate structures might be attributed to the high interference density between the layers. These enhancements in nanolaminate structure could enable a new category of dielectric materials with high energy storage density and high relative permittivity. Therefore, nanolaminate technology can be used as a new technique to develop advanced functionality of materials by promoting combined interactions among organized components [1].

Figure 9

3. Nanolaminates properties for high performance energy storage devices

Dielectric materials with different structures are being studied to obtain unique physical, chemical and mechanical properties with a large dielectric constant. These are intended for a broad range of applications that include random access memory, capacitors and tunable devices. Although metal oxides have a high dielectric constant, they usually have a narrow band gap, which leads to a large leakage current of a dielectric. Most materials with high dielectric constant are also thermodynamically unstable when they are in contact with a silicon wafer or electrodes [118]. Therefore, investigations have worked to improve the thermal stability and decrease the leakage current of metal oxide dielectrics by employing additives [8-11]. However, this approach may result in a decrease in composite dielectric constants due to low permittivity values of the additives. Thus, the new composites might be not suitable for use in electronic devices [8-11].

New fabrication methods toward miniaturized dielectrics with ultrathin layered structures with different compounds are being investigated by using sputtering and vapor deposition methods. For instance, since the use of inorganic hybrid material structures is limited in applications requiring flexibility, nanolaminate structures consisting of polymer and metal oxide layers are being investigated [10, 23, 119]. Table 3 shows the composition and performance of combined polymer and metal oxide composites with different structures that were synthesized using different methods. The silicone/Al_2O_3 nanolaminate composites synthesized by plasma enhanced chemical vapor

Journal of Materials Chemistry A Accepted Manuscript

deposition (PECVD) revealed a breakdown field more than 5 MV/cm and the leakage current was strongly affected by the thickness of the individual Al_2O_3 layers [120].

It was also estimated that excellent performance was obtained for the fabricated nanolaminates when the Al_2O_3 layers were more than 10 nm thick. Petal et al. [120] indicated that the leakage current density at a field strength of 1 MV/cm was $\sim 10^{-9}$ A/cm^2 for a nanolaminate composite. This performance suggests that a nanolaminate structure was effective for microelectronic and energy storage applications.

Table 3

3.1. Electrical characterization and dielectric properties of metal oxide nanolaminates

High dielectric constant metal oxide nanolayers such as ZrO_2, Ta_2O_5, Nb_2O_5, TiO_2, HfO_2, and Al_2O_3 are being actively pursued for applications in nanoelectronics devices to increase the charge storage capability of dielectric layers [1, 27]. Among these metal oxide compounds, TiO_2 [121], HfO_2 [87] and Al_2O_3 [27] have been widely studied as candidates to replace SiO_2 thin films due to their high dielectric constant, good thermodynamic stability with silicon, large band gap and high resistance [27, 87, 121]. Despite the advantages of these metal oxides, however, TiO_2 thin films exhibit a relatively large leakage current due to its small energy band gap [121].

Materials such as HfO_2, however, could not be crystallized at low temperature, which results in a high leakage current along the grain boundaries [87]. As well, the low relative dielectric constant of Al_2O_3 is a disadvantage for using this compound in dielectrics [27]. Kukli et al. [27] have suggested that these transition metal oxides could be well insulated dielectrics if an appropriate stoichiometry was obtained. However, obtaining an ideal stoichiometry for a metal oxide was complicated due to the creation of fully oxidized metals during the low-temperature film deposition process. Thus, doped thin films and nanolaminate structures using multicomponent oxides have been investigated to complement the limitations of these metal oxide dielectric thin films [121].

Jõgi et al. [52] fabricated Al_2O_3/TiO_2 thin film mixtures and nanolaminates for thin film electroluminescence displays using atomic layer deposition. The dielectric properties of these two structures were compared. Both $Al_xTi_yO_z$ mixtures and Al_2O_3-TiO_2-Al_2O_3 laminate structures possess higher leakage currents than pure Al_2O_3 at comparable oxide thickness values when silicon and low work function electrodes were used. It was suggested that the properties of the laminate structure were more predictable due to better control of the layers. In the case of laminate structures, breakdown voltages and leakage currents were also monotonically dependent on the layer thicknesses [52]. There is scope to further optimize, the Al:Ti atomic ratios in the mixture films of

Journal of Materials Chemistry A Accepted Manuscript

$Al_xTi_yO_z$ and, as well, the influence on the work function and interfacial barriers in the composite structure needs to be studied [52].

Li et al. [56] explained why Al_2O_3/TiO_2 nanolaminate structures present a high dielectric constant (~1,000) through simulating an equivalent circuit composed of two parallel resistor-capacitor (*RC*) elements connected in series. The resistance and capacitance of Al_2O_3 and TiO_2 sublayers were assumed as R_1, C_1 and R_2, C_2, respectively. The capacitance of the Al_2O_3/TiO_2 nanolaminates can be stated as:

$$C = \frac{C_\infty + (C_0 - C_\infty)}{[1+(\omega\tau)^2]} \qquad (1)$$

where C_0 and C_∞ are expressed as :

$$C_0 = \frac{(C_1 R_1^2 + C_2 R_2^2)}{(R_1+R_2)^2} \;,\quad C_\infty = \frac{C_1 C_2}{(C_1+C_2)} \qquad (2)$$

The dielectric constant (ε) of the nanolaminates can be estimated by C_0 at low frequency [56]. The dielectric constant of Al_2O_3/TiO_2 nanolaminates would according to this theoretical analysis range from 3 to 750 times larger than that of Al_2O_3 [56]. It was suggested that the true dielectric constant of this nanolaminate structure could not be so high because the structures exhibit leakage when the sublayers become thinner; which is a result of electron hopping in the TiO_2 sublayers [56].

The interfacial layer thickness that is generated can also be calculated by the formula for the total capacitance in the series model. Kim et al. [121] reported that the dielectric constant of synthesized Al_2O_3-TiO_2-Al_2O_3 decreased when the nanolaminate was annealed at 600 °C due to the increased interfacial layer that included SiO_x in the interface of the Si/Al_2O_3-TiO_2-Al_2O_3 films. It was observed that the formation of a metal oxide composite nanolaminate and an interfacial layer influenced the dielectric constant as well as the leakage current. This model also shows that the dielectric properties of metal oxide composites with nanolaminate structures are more predictable.

3.2. Al_2O_3 nanolaminate structure and post-deposition annealing effects

An insulated material with intermediated thickness layers and high dielectric constant provides high gate capacitance in a microelectronic device. However, other required specifications such as leakage currents, high breakdown fields and good thermodynamic stability must also be fulfilled.

Journal of Materials Chemistry A Accepted Manuscript

High permittivity dielectrics that could replace SiO_2 as gate insulators in microelectronic devices [1, 27, 56] have been investigated. It is also necessary to have a manufacturing technique capable of producing high quality thin films with good dielectric properties, accurate control of the thickness and uniformity over a large area [57].

Aluminum oxide (Al_2O_3) is widely used in microelectronic devices. It has replaced SiO_2 due to its intrinsic properties of a high dielectric constant ($\varepsilon_r = 9$), low leakage current, and high breakdown voltage (9 MV/cm) [1, 27, 56]. The dielectric properties of Al_2O_3 films are influenced by its crystal structure that exhibits more than 20 different phase structures [122]. However, the most common structures for Al_2O_3 are α-Al_2O_3, γ-Al_2O_3, θ-Al_2O_3 and κ-Al_2O_3 [123]. The dielectric properties of Al_2O_3 are also affected by the preparation technique; especially the deposition rate in evaporated films [124]. Investigations on the fabrication of Al_2O_3 nanolayers by deposition techniques [27, 56, 124] have been performed to obtain better control of the phase formation as well as dielectric properties.

Recently Prasanna et al. [124] reported on Al_2O_3 nanolayers that were deposited onto silicon substrates by a DC magnetron sputtering method. The compositions of the fabricated nanolaminates were studied using XPS analysis and the as-deposited nanolayers were found to be oxygen rich with an O/Al atomic ratio of 1.72. Furthermore, the Al_2O_3 nanolaminate films were amorphous after annealing at a temperature greater than 750 °C. The nanolaminate structure might be broken and mixed, as well as given a single dielectric layer with moderate dielectric properties. The root mean square roughness of the nanolaminates was found to decrease with post-deposition annealing [124]. A minimum value of 0.73 nm was observed with an increase in annealing temperature to 750 °C [124]. It was found that a Al-Al_2O_3-Al thin film capacitor fabricated on a silicon substrate exhibited a dielectric constant of 15 at a frequency of 1 kHz [124]. This dielectric constant was calculated by referring to capacitance (C), film thickness (d), permittivity of free space (ε□) and the area of the capacitor, using the relationship formula below:

$$\varepsilon_r = \frac{Cd}{\varepsilon_\circ A} \qquad (3)$$

The capacitance decreased with increasing frequency and was attributed to interfacial polarization in the nanolaminate structure. The alternating current conductivity of the fabricated capacitor was calculated on the basis of the following relationship [124].

Journal of Materials Chemistry A Accepted Manuscript

$$\sigma = 2\pi f \ tan\delta \varepsilon_r \varepsilon_\circ \quad (4)$$

3.3. Novel mixed metal phosphonate nanolaminates for high dielectric composite materials

Dielectric capacitors that have desirable attributes portable electronic devices, such as energy density, power density and rate capability; are not available and under current investigation [125]. The energy density of a dielectric capacitor can be calculated from [125]:

$$W = 0.5\varepsilon_0 \varepsilon_r E_{bd}^2 \quad (5)$$

where ε_r is relative dielectric permittivity, ε_0 is 8.854×10^{-12} F/m and E_{bd} is the dielectric breakdown field strength.

The energy density equation indicates that dielectric materials should demonstrate a high potential breakdown field strength in order to increase their energy density. Polymers exhibit high values of dielectric breakdown field strength (E_{bd}) [125]. In addition to this, polymers are processible, which is another advantage. However, the dielectric constants for polymers are frequently low [125].

Investigations [126, 127] have been performed on polymers and high dielectric constant materials, such as barium titanate ($BaTiO_3$), in order to obtain a composite containing a high dielectric constant combined with a large dielectric breakdown field strength. The, results showed poor dispersion of $BaTiO_3$ in the polymer matrix due to the high filler loadings of $BaTiO_3$. This poor dispersion may accrue in lower permittivity values that can be predicted on the basis of various theoretical models of composite dielectrics. Kim et al. [128] modified the surface of $BaTiO_3$ using several organo-phosphonic acids to increase the dispersion of inorganic ceramic materials in the polymer matrix. This modification led to a better dispersion with a high effective dielectric constant. However, the E_{bd} value was still 50% lower than that of the pure polymer matrix.

Barber et al. [125] investigated mixed metal phosphonates consisting of a 1:1 ratio of divalent to tetravalent metal cations. The components of $BaTi(C_6H_5PO_3)_3$ and $SrTi(C_6H_5PO_3)_3$ were synthesized using a hydrothermal method. These mixed metal phosphonate compounds consist of $BaTiO_3$ or $SrTiO_3$ in a phenyl phosphonic acid ($C_6H_5PO_3H_2$), Figure 10. The dielectric properties of the synthesized mixed metal phosphonates loaded in a 40 wt.% polystyrene matrix were measured, Table 4. It can be seen that incorporation of two metals into the phosphonate structure such as $BaTi(C_6H_5PO_3)_3$ and $SrTi(C_6H_5PO_3)_3$ enhanced the dielectric constant. The dielectric constant of

Journal of Materials Chemistry A Accepted Manuscript

$SrTi(C_6H_5PO_3)_3$ was 66% higher than that of $SrTiO_3$ and the dielectric constant of $BaTi(C_6H_5PO_3)_3$ was 106% higher than that of $BaTiO_3$ [125].

It was observed that the dielectric constant of a single metal phosphonate such as $Ba(C_6H_5PO_3)_3.H_2O$ or $Ti(C_6H_5PO_3)_2$ at the same loading of 40 wt.% in a polystyrene matrix was significantly lower than the values for $BaTiO_3$ in polystyrene, or $BaTi(C_6H_5PO_3)_3$ in polystyrene [125]. This enhancement of the dielectric constant in the two metal mixed phosphonate structures relative to single metal phosphonate depended on the presence of the two different metals joined by an attachment atom in the inorganic phase [125]. Further exploration in this area is needed to obtain composite structures with enhanced dielectric properties.

Figure 10

Table 4

3.4. Development on artificial ferroelectric nanolaminates for energy storage devices

Dielectric properties of perovskite materials play a critical role in many electronic devices, such as energy storage, capacitors and memory devices [1]. Therefore, widespread research has been directed at distinguishing novel dielectric materials or exploring new properties in known perovskite materials. Some recent researches determined a number of layered perovskites which illustrated high dielectric constant and ferroelectric properties [129-130]. In addition, perovskite materials with nanolaminate geometries may be critical for obtaining optimal performance with high storage density [131]. It also has been seen that dielectric constants of perovskite thin films are one order of magnitude smaller than those of their bulk [132, 133]. Therefore, many theoretical and experimental studies have been directed toward understanding the detrimental characteristics of nanolaminate geometry [131, 133, 134]. Recently Osada et al. [134] fabricated a new class of $Ca_2Nb_3O_{10}$ thin films based on perovskite nanolaminates. Growth of the nanolaminates with a good interface quality led to films showing high dielectric constant (>200) and low leakage current density ($<10^{-7}$ A/cm^2) in the films with thickness down to 10 nm and less than 5 nm, respectively [134]. These results illustrate that perovskite nanolaminate may create new possibilities for applications ranging from electronics to energy storage devices. Generally, 2D nanosheets and nanolaminates, for example ceramic/graphene, will thus become an important research target for high power applications and many research works in this area are underway.

Journal of Materials Chemistry A Accepted Manuscript

4. Summary

This work presented a review of dielectric materials for electronic and energy storage devices synthesized by deposition technique. Key material considerations discussed include: permittivity, band gap, thermodynamic stability of silicon substrate, interface quality, film morphology etc. Oxide nanolaminates provide an ideal model for studying dielectric phenomena in nanosheet systems. Dielectric constant and sublayer effects on amorphous Al_2O_3 and monoclinic HfO_2 showed that dielectric constant value increased and it was larger than the calculated value in the series model when the sublayer thickness decreased in nanolaminate films. This increase in the dielectric constant in the fabricated Al_2O_3/HfO_2 nanolaminate films was attributed to the appearance of a tetragonal phase structure in the HfO_2 sublayer with a higher dielectric constant than that of HfO_2 with monoclinic phase. In addition, the effect of dopant and potentially high dielectric constant on the dielectric nanolaminates was reviewed. Dielectric nanolaminate materials with high potential dielectric strength (E_{BD}) combined with high dielectric permittivity (ε_r) (e.g. $BaTiO_3$ in P(VDF-HFP)) were discussed as potential materials for high performance energy storage systems. The synthesized uniform films demonstrated that E_{BD} of the nanolaminates increased 2.5 times in comparison to the unfilled polymer. This improvement in breakdown strength for the nanolaminate structures might be attributed to the high interference density between the layers. Dielectric properties of perovskite nanolaminates with inorganic structure also showed that a large dielectric constant and low leakage current can be seen in these structures with nanolayers. Therefore, these materials with two-dimensional structure have potential to be used in next generation nanoelectronics. All these developments of novel nanolaminates demonstrated how to handle and process nanosheets materials and develop nanotechnology in general.

5. Acknowledgements

The authors acknowledge financial support through the Australia-India Strategic Research Fund (AISRF) ST060048. The authors thank Dr Mostafa Nikzad in developing the conceptual illustrations.

6. References

1. M. Osada and T. Sasaki, *Adv. Mater.*, 2012, **24**, 210-228.
2. M. Osada and T. Sasaki, *J. Mater. Chem.*, 2009, **19**, 2503-2511.
3. R. Z. Ma and T. Sasaki, *Adv. Mater.*, 2010, **22**, 5082-5104.
4. G. D. Wilk, R. M. Wallance and J. M. Anthony, *J. Appl. Phys.*, 2001, **89**, 5243-5275.
5. R. M. Wallace and G. Wilk, *MRS Bul.*, 2002, **27**, 192-197.

Journal of Materials Chemistry A Accepted Manuscript

6. P. W. Peacock and J. Robertson, *J. Appl. Phys.*, 2002, **92**, 4312-4321.

7. D. G. Schlom and J. H. Haeni, *MRS Bull.*, 2002, **27**, 198-204.

8. W. J. Zhu, T. Tamagawa, M. Gibson, T. Furukawa and T. P. Ma, *IEEE Electron Device Lett.*, 2002, **23**, 649-651.

9. M. S. Joo, B. J. Cho, C. C. Yeo, N. Wu, H. Yu, C. Zhu, M. F. Li, D. L. Kwong, N. Balasibramanian, *Jpn. J. Appl. Phys. Part 2*, 2003, **42**, L220-L222.

10. M. H. Cho, Y. S Roh, C. N. Whang, K. Jeong, H. J. Choi, S. W. Nam, D. H. Ko, J. H. Lee, N. I. Lee, K. Fujihara, *Appl. Phys. Lett.*, 2002, **81**, 1071-1073.

11. H. S. Chang, S. Jeon, H. Hwang. D. W. Moon, *Appl. Phys. Lett.*, 2002, 80, 3385-3387.

12. S. Jeon, H. Yang, D. G. Park, H. Hwang, *Jpn. J. Appl. Phys. Part 1*, 2002*,* ***41***, 2390-2393.

13. T.W. Barbee, *IEEE Aerospace Conference Proceedings*, 2003, **1-8**, 1745-1754.

14. A. I. Kingon, S. K. Streiffer, C. Basceri, S. R. Summerfelt, *MRS Bull.*, 1996, **21**, 46-52.

15. A. Kingon, *Nature*, 1999, **401**, 658-659.

16. A. I. Kingon, J. P. Maria, S. K. Streiffer, Nature, 2000, **406**, 1032-1038.

17. S. K. Kim, S. W. Lee, J. H. Han, B. Lee, S. Han, C. S. Hwang, *Adv. Funct. Mater.* 2010, **20**, 2989-3003.

18. J. Niinistö, K. Kukli, M. Heikkilä, M. Ritala, M. Leskelä, *Adv. Eng. Mater.* 2009, **11**, 223-34.

19. E. K. Akdogan, W. Mayo, A. Safari, *Advances in Dielectric Ceramics*, 88 Nair, K. M., Bhalla, A. S.; Westerville, OH, The American Ceramic Society, 1998.

20. G. L. Brennecka, J. F. Ihlefeld, J. P. Maria, B. A. Tuttle, P. G. Clem, *J. Am. Ceram. Soc.* 2010, **93**, 3935-3954.

21. G. D. Wilk, R. M. Wallace, J. M. Anthony, *J. Appl. Phys.*, 2001, **89**, 5243-5275.

22. J. Robertson, *Rep. Prog. Phys.*, 2006, **69**, 327-396.

23. R.P. Ortiz, A. Facchetti, T. J. Marks, *Chem. Rev.*, 2010, **110**, 205-239.

24. I. Burn, D. M. Smyth, *J. Mater. Sci.* 1972, **7**, 339-&.

25. P. Barber, S. Balasubramanian, Y. Anguchamy, S. Gong, A. Wibowo, H. Gao, H. J. Ploehn, H. C. Zur Loye, *Materials*, 2009, 2, 1697-1733.

26. R. J. Cava, *J. Mater. Chem.* 2001, **11**, 54-62.

27. K. Kukli, M. Ritala, M. Leskelä, *J. Electrochem. Soc.*, 2001, **148**, F35-F41.

28. M. Kadoshima, M. Hiratani, Y. Shimamoto, K. Torii, H. Miki, S. Kimura, T. Nabatame, *Thin Solid Films*, 2003, **424**, 224-228.

29. S. K. Kim, W. D. Kim, K. M. Kim, C. S. Hwang, J. Jeong, *Appl. Phys. Lett.* 2004, **85**, 4112-4114.

30. R. J. Cava, J. J. Krajewski, W. F. Peck Jr, G. L. Roberts, *J. Mater. Res.*, 1996, **11**, 1428-1432.

Journal of Materials Chemistry A Accepted Manuscript

31. J. R. Jameson, P. B. Griffin, A. Agah, J. D. Plummer, H. S. Kim, D. V. Taylor, P. C. McIntyre, W. A. Harrison, *IEEE*, 2003, 91-94.

32. J. W. McPherson, J. Kim, A. Shanware, H. Mogul, J. Rodrigues, *J. IEEE Tran. Elec. Dev.*, 2003, **50**, 1771-1778.

33. G. L. Brennecka, J. F. Ihlefeld, J. P. Maria, B. A. Tuttle, P. G. Clem, *J. Am. Ceram. Soc.*, 2010, **93**, 3935-3954.

34. K. Kukli, M. Ritala, M. Leskelä, *Nonstruc. Mater.*, 1997, **8**, 785-793.

35. I. Jõgi, K. Kukli, M. Ritala, M. Leskelä, J. Aarik, A. Aidla, J. Lu, *Microelectronic Eng.*, 2010 **87**, 144-149.

36. M. A. Subramanian, D. Li, N. Duan, B. A. Reisner, A. W. Sleight, *J. Solid State Chem.*, 2000, **151**, 323-325.

37. J. W. Elam, Z. A. Sechrist, S. M. George, *Thin Solid Films*, 2002, **414**, 43-55.

38. J. M. Jensen, A. B. Oelkers, R. Toivola, D. C. Johnson, J. W. Elam, S. M. George, *Chem. Mater.*, 2002, **14**, 2276-2282.

39. Z. A. Sechrist, F. H. Fabreguette, O. Heintz, T. M. Phung, D. C. Johnson, S. M. George, *Chem. Mater.*, 2005, **17**, 3435-3485.

40. S. J. Veprek, *J. Vac. Sci. Technol. A* 1999, **17**, 2401-2420.

41. P. C. Yashar, W. D. Sproul, *Vacuum* 1999, **55**, 179-190.

42. G. Chen, M. Neagu, *Appl. Phys. Lett.* 1997, **71**, 2761-2763.

43. G. Chen, *Phys. Rev. B*, 1998, **57**, 14958-14973.

44. H. B. Huang, F. Spaepen, *Acta Mater.* 2000, **48**, 3261-3269.

45. J. H. Lee, Y. S. Kim, H. S. Jung, J. H. Lee, N. I. Lee, H. K. Kang, J. H. Ku, H. S. Kang, Y. K. Kim, K. H. Cho, K. P. Sub, *VLSI Tech. Dig. IEEE Cat. No. 02CH37302*, 2002, **84**.

46. Y. N. Tan, W. K. Chim, W. K. Choi, M. S. Joo, T. H. Ng, B. J. Cho, *IEDM Tech. Dig. IEEE Cat. No. 04CH37602*, **889**, 2004.

47. T. E. Seidel, A. Srivastava, Z. Zhang, T. Dimitrova, A.R. Londergan, Z. Karim, *ECS Symposium*, 2005, **1**, 107.

48. S. Y. Kim, *IEEE IEDM Tech. Dig.* 2006, **871**.

49. W. Li, Z. Chen, R. N. Premnath, B. Kabius, O. Auciello, *J. Appl. Phys.*, 2011, **110**, 024106.

50. E. Miranda, J. Sune, T. Das, C. Mahata, C. K. Maiti, *J. Appl. Phys.*, 2012, **112**, 064113.

51. S. J. Ding, J. Xu, Y. Huang, Q. Q. Sun, D. W. Zhang, M. F. Li, *J. Appl. Phys.*, 2008, **103**, 092909.

52. I. Jõgi, K. Kukli, M. Kemell, M. Ritala, M. Leskelä, *J. Appl. Phys.*, 2007, **102**, 114114.

Journal of Materials Chemistry A Accepted Manuscript

53. M. Osada, Y. Ebina, H. Funakubo, S. Yokoyama, T. Kiguchiu, K. Takada, T. Sasaki, *Adv. Mater.*, 2006, **18**, 1023-1027.
54. B. M. Knez, K. Nielsch, L. Niinist□, *Adv. Mater.*, 2007, **19**, 3425-38.
55. S. J. Ding, M. Zhang, W. Chen, D. W. Zhang, L. K. Wang, X. P. Wang, C. Zhu, M. F. Li, *J. Appl. Phys.* 2006, **88**, 042905.
56. W. Li, O. Auciello, R. N. Premnath, B. Kabius, *Appl. Phys. Lett.*, 2010, **96**, 162907.
57. R. Advincula, W. Knoll, *Functional Polymer Films,* Wiley, 2011.
58. B. S. Ong, K. L. Pey, C. Y. Ong, C. S. Tan, D. A. Antoniadis, E. A. Fitzgerald, *Appl. Phys. Lett.*, 2011, **98**, 182102-182104.
59. M. Leskelä, M. Ritala, *Angew. Chem. Int. Ed.*, 2003, **42**, 5548-54.
60. L. Niinist□, J. Päiväsaari, J. Niinist□, M. Putkonen, M. Nieminen, *Phys. Status Solidi A*, 2004, **201**, 1443-1452.
61. H. Kim, *J. Vac. Sci. Technol. B*, 2003, **21**, 2231-2261.
62. R. Puurunen, *J. Appl. Phys.*, 2005, **97**, 121301.
63. M. C. Cisneros-Morales, C. R. Aita, *J. Appl. Phys.*, 2012, **111**, 109904.
64. E. Guziewicz, M. Godlewski, L. Wachnicki, T. A. Krajewski, G. Luka, S. Gieraltowska, R. Jakiela, A. Stonert, W. Lisowski, M. Krawczyk, J.W. Sobczak, A. Jablonski, *Semicond. Sci. Technol.*, 2012, **27**, 074011.
65. X. Sun, M. Xie, G. Wang, H. Sun, A. S. Cavanagh, A. S., J. J. Travis, S. M. George, J. Lian, *J. Electro. Soc.*, 2012, **159**, A364-A369.
66. G. Dingemans, M. C. M. Van de Sanden, W. M. M. Kessels, *J. Electro. Soc.*, 2010, **13**, H76-H79.
67. W. R. Grove, *Phil. Trans. R. Soc. Lond.*, 1852, **142**, 87-101.
68. M. Panjan, T. Peterman, M. Čekda, P. Panjan, *Surf. Coat. Tech.*, 2009, **204**, 850-853.
69. T. Wan, H. Aoki, J. Hikawa, J. H. Lee, *Biomed. Mat. and Eng.*, 2007, **17**, 291-297.
70. M. T. Greiner, L. Chai, M. G. Helander, W. M. Tang, Z. H. Lu, *Adv. Funct. Mater.*, 2013, **23**, 215-226.
71. C. H. Heo, S. B. Lee, J. H. Boo, *Thin Solid Films*, 2005, **435**, 183-188.
72. R. M. Wallace, G. D. Wilk, *Crit. Rev. Solid State Mater.*, 2003, **28**, 231-285.
73. R. M. Wallace, G. Wilk, *MRS Bull.*, 2002, **27**, 186-187.
74. R. Wallace, O. Auciello, *Multifunctional Thin Films Book Series,* O. Auciello, R. Ramesh, Eds.; Springer: New York, 2005, p 79-126.
75. G. Lee, B. K. Lai, C. Phatak, R. S. Katiyar, O. Auciello, *J. Appl. Phys.*, 2013, **114**, 027001.

Journal of Materials Chemistry A Accepted Manuscript

76. T. Sasaki, M. Watanabe, H. Hashizume, H. Yamada, H. Nakazawa, *J. Am. Chem. Soc.*, **1996**, 118, 8329-8335.

77. T. Sasaki, M. Watanabe, *J. Am. Chem. Soc.*, 1998, **120**, 4682-4689.

78. T. Tanaka, Y. Ebina, K. Takada, K. Kurashima, T. Sasaki, *Chem. Mater.*, 2003, 15, 3564-3568.

79. C. J. F□rst, C. R. Ashman, K. Schwarz, P. E. Bl□ch, *Nature*, 2004, 427, 53-56.

80. M. Gutowski, J. E. Jaffe, C. L. Liu, M. Stoker, R. I. Hegde, R. S. Rai, P. J. Tobin, *Appl. Phys. Lett.*, 2002, **80**, 1897-1899.

81. Y. Omomo, T. Sasaki, L. Z. Wang, M. Watanabe, *J. Am. Chem. Soc.*, 2003, **125**, 3568-3575.

82. O. Aucielle, W. Fan, B. Kabius, S. Saha, J. A. Carlisle, R. P. H. Chang, C. Lopez, E. A. Irene, R. A. Baragiola, *Appl. Phys. Lett.*, 2005, **86**, 042904.

83. H. Y. Yu, M. F. Li, B. J. Cho, C. C. Yeo, M. S. Joo, D. L. Kwong, J. S. Pan, C. H. Ang, J. Z. Zheng, S. Ramanathan, *Appl. Phys. Lett.*, 2002, **81**, 376-378.

84. F. El Kamel, P. Gonon, C. Vallee, *Appl. Phys. Lett.*, 2007, **91**, 172909.

85. D. Fuchs, C. W. Schneider, R. Schneider, H. Rietschel, *J. Appl. Phys.*, 1999, **85**, 7362-7369.

86. W. Li, O. Auciello, R. Premnath, B. Kabius, *Appl. Phys. Lett.*, 2010, **96**, 162907.

87. P. K. Park, E. S. Cha, S. W. Kang, *Appl. Phys. Lett.*, 2007, **90**, 232906.

88. F. A. Modine, D. Lubben, J. B. Bates, *J. Appl. Phys*., 1993, **74**, 2658.

89. P. C. Yashar, S. A. Barnett, L. Hultman, W. D. Sproul, *J. Mater. Res.*, 1999, **14**, 3614-3622.

90. D. Schwenk, F. Fishman, F. Schwabl, *Phys. Rev. B*, 1988, **38**, 11618-11638.

91. G. Chen, M. Neagu, *Appl. Phys. Lett.*, 1997, **71**, 2761-2763.

92. J. Patscheider, N. Hellgren, R. T. Haasch, I. Petrov, J. E. Greene, *Phys. Rev. B*, 2011, **83**, 125124

93. C. E. Kim, I. Yun, *App. Surf. Sci.*, 2012, **258**, 3089-3093.

94. Z. Tang, X. Zhu, H. Xu, Y. Xia, J. Yin, Z. Liu, A. Li, F. Yan, *Mater. Lett.*, 2013, **92**, 21-24.

95. A. R. Chaudhuri, A. Fissel, V. R. Archakam, H. J. Osten, *Appl. Phys. Lett.*, 2013, **102**, 022904.

96. J. T. Anderson, C. L. Munsee, C. M. Hung, T. M. Phung, G. S. Herman, D. C. Johnson, J. F. Wagner, D. A. Keszler, *Adv. Funct. Mater.*, 2007, **17**, 2117-2124.

97. I. Jõgi, A. Tamm, K. Kukli, M. Kemell, J. Lu, T. Sajavaara, M. Ritala, M. Leskel□, *J. Elect. Soc.*, 2010, **157**, G202-G210.

98. C. H. Choi, S. J. Rhee, T. S. Jeon, N. Lu, J. H. Sim, R. Clark, M. Niwa, D. L. Kwong, *Rech. Dig. -Int. Electron Devices Meet.*, 2002, 857.

99. X. P. Wang, M. F. Li, A. Chin, C. X. Zhu, J. Shao, W. Lu, X. C. Shen, X. F. Yu, R. Chi, C. Shen, A. C. H. Huan, J. S. Pan, A. Y. Du, P. Lo, D. S. H. Chan, D. L. Kwong, *Solid-State Electron.*, 2006, **50**, 986-991.

Journal of Materials Chemistry A Accepted Manuscript

100. G. Dutta, K. P. S. Hembram, G. M. Rao, U. Waghmare, *Appl. Phys. Lett.*, 2006, **89**, 202904.

101. K. Chu, M. L. Chang, M. L. Steigerwald, R. M. Fleming, R. L. Opila, R. B. van Dover, C. D. W. Jones, *J. Appl. Phys.* 2002, **91**, 308-316.

102. V. Mikhelashvili, G. Eisenstein, *Thin Solid Films*, 2006, **515**, 346-352.

103. K. Kukli, M. Ritala, M. Leskelä, J. Sundqvist, L. Oberbeck, J. Heitmann, U. Schr□der, J. Aarik, A. Aidla, *Thin Solid Films*, 2007, **515**, 6443-6451.

104. R. K. Grubbs, C. E. Nelson, N. J. Steinmetz, S. M. George, *Thin Solid Films*, 2004, **467**, 16-27.

105. W. F. A. Besling, E. Young, T. Conard, C. Zhao, R. Carter, W. Vandervorst, M. Caymax, S. De Gendt, M. Heyns, J. Maes, M. Tuominen, S. Haukka, *J. of Non-Crystalline Solids*, 2002, **303**, 123-133.

106. H. Kattelus, M. Ylilammi, J. Saarilahti, J. Antson, S. Lindfors, *Thin Solid Films*, 1993, **225**, 296-298.

107. K. Kukli, J. Ihanus, M. Ritala, M. Leskela, *J. Electrochem. Soc.*, 1997, **144**, 300-306.

108. J. W. Elam, S. M. George, *Chem. Mater.*, 2003, **13**, 1020-1028.

109. T. Roessler, J. Gluch, M. Albert, J. W. Bartha, *Thin Solid Film*, 2010, **518**, 4680-4683.

110. K. Kukli, J. Ihanus, M. Ritala, M. Leskela, *Appl. Phys. Lett.*, 1996, **68**, 3737-3739.

111. K. Kukli, M. Ritala, M. Leskela, T. Sajavaara, J. Keinonen, D. Gilmer, S. Bagchi, L. Prabhu, *J. of Non-Crystalline Solids*, 2002, **303**, 35-39.

112. S. P. Fillery, H. Koerner, L. Drummy, E. Dunkerley, M. F. Durstock, D. F. Schmidt, R. A. Vaia, *ACS Appl. Mater. Interfaces*, 2012, **4**, 1388-1396.

113. S. S. Brandstetter, L. F. Drummy, J. C. Horwath, D. L. Schweikart, R. A. Vaia, *IEEE Trans. Dielectr. Electr. Insul.*, 2008, **15**, 287-290.

114. Y. Cao, P. C. Irwin, K. Younsi, *IEEE Trans. Dielectr. Electr. Insul.*, 2004, **11**, 797-807.

115. P. Kim, X. H. Zhang, B. Domercq, S. C. Jones, P. J. Hotchkiss, S. R. Marder, B. Kippelen, J. W. Perry, *Appl. Phys. Lett.*, 2008, **93**, 013302.

116. P. Kim, M. N. Doss, J. P. Tillotson, P. J. Hotchkiss, M. J. Pan, S. R. Marder, J. Li, J. P. Calame, J. W. Perry, *ACS Nano*, 2009, **3**, 2581-2592.

117. J. Li, S. I. Soek, B. Chu, F. Dogan, Q. Zhang, Q. Wang, *Adv. Mater.*, 2009, 21, 217-221.

118. Y. Aoki, T. Kunitake, *Adv. Mater.*, 2004, **16**, 118-123.

119. G. Dennler, C. Lungenschmied, H. Neugebauer, N. S. Sariciftci, M. Latrèche, G. Czeremuszkin, M. R. Wertheimer, *Thin Solid Films*, 2006, **349**, 511-512.

120. R. P. Patel, D. Chiavetta, C. A. Wolden, *J. Vac. Sci. Technol. A*, 2011, **29**, 061508.

121. C. E. Kim, I. Yun, *Applied Surface Science*, 2012, **258**, 3089-3093.

Journal of Materials Chemistry A Accepted Manuscript

122. W. H. Gitzen, *Alumina as a Ceramic Material*, Eds.; Westerville OH, The American Ceramic Society,1970, p3.

123. O. Zywitzki, G. Hoetzsch, *Surface and Coatings Technology*, 1996, **86-7**, 640-647.

124. S. Prasanna, G. Krishnendu, S. Shalini, P. Biji, G. Mohan Rao, S. Jayakumar, R. Balasundaraprabhu, *Materials Science in Semiconductor Processing*, In press, 2013.

125. P. Barber, H. Houghton, S. Balasubramanian, Y. K. Anguchamy, H. J. Ploehn, H. C. Zur Loye, *Chem. Mater.*, 2009, **21**, 1303-1310.

126. Y. Cao, P. C. Irwin, K. Younsi, *IEEE Trans. Dielectr. Electr. Insul.*, *2004*, 11, 797-807.

127. W. J. Sarjeant, *Handbook of Low and High Dielectric Constant Materials and Their Applications,* H. S. Nalwa, Eds.; Academic Press: San Diego, 1999, p 423–491.

128. P. Kim, S. C. Jones, P. J. Hotchkiss, N. Haddock, B. Kippelen, S. R. Marder, J. W. Perry, *Adv. Mater.*, 2007, 19, 1001–1005.

129. C. A. P. deAruj, J. D. Cuchiaro, L. D. McMillan, M. C. Scott, J. F. Scott, *Nature*, 1995, **374**, 627-629.

130. M. A. Subramanian, D. Li, N. Duan, B. A. Reisner, A. W. Sleight, *J. Solid State Chem.*, 2000, **151**, 3230325.

131. M. Osada, T. Sasaki, *Int. J. Appl. Ceram. Technol.*, 2012, **9**, 29-36.

132. C. S. Hwang, *J. Appl. Phys.* 2002, **92**, 432-437.

133. L. J. Sinnamon, M. M. Saad, R. M. Bowman, J. M. Gregg, *Appl. Phys. Lett.*, 2002, **81**, 703-705.

134. M. Osada, K. Akatsuka, Y. Ebina, H. Funakubo, K. Ono, K. Takada, T. Sasaki, *ACS Nano*, 2010, **4**, 5225-5232.

Journal of Materials Chemistry A Accepted Manuscript

FIGURE CAPTIONS:

Figure 1. Polarization of a dielectric in an external electric field ($\vec{E}$: external electric field, d: dielectric distance and σ_i: surface charge density).

Figure 2. A schematic, on the left hand side, that illustrates the materials design of a Al_2O_3/ZnO nanolaminate. The right hand side shows a cross sessional transmission electron micrograph of a Al_2O_3/ZnO nanolaminate where the layer thickness is about 30 nanometers. Reproduced from data published in ref. 37.

Figure 3. A schematic illustration of an ALD process for synthesizing thin film layers where an iterative, continuous deposition cycle is indicated.

Figure 4. Schematics of: (a) 2 dimensional oxide nanosheets. Reproduced from data published in ref. 1, and (b) diagram for synthesis of a thin film by magnetron sputtering.

Figure 5. A schematic for a multilayered organic electronic device and a metal oxide shield layer. Reproduced from data published in ref. 70.

Figure 6. (a) A schematic of the Al_2O_3 and TiO_2 nanolaminates, (b) titanium and aluminium elemental maps obtained from energy filtered TEM images, and (c) bright field TEM image of AlO_x/TiO_y nanolaminates. Adapted from data published in ref. 49.

Figure 7. (a) Effect of sublayer thickness on dielectric constant of HfO_2/Al_2O_3 nanolaminate films before and after annealing, and (b) TEM image (cross-sectional) of HfO_2 (dark layers)/Al_2O_3 (bright layers) nanolaminate film with thickness of 10 Å. Adapted from data published in ref. 87.

Figure 8. Improvement of dielectric constant and leakage current density of the perovskite nanolaminate by doping and modifying the structure. Adapted from data published in ref. 1.

Figure 9. (a) A schematic for designing materials *via* nanoarchitectonics of dielectric nanosheets, and (b) Schematic cross sectional image of $(LaNb_2O_7/Ca_2Nb_3O_{10})_3$ nanolaminates. Reproduced from data published in ref. 1.

Figure 10. A schematic of the mixed metal phosphonate structure. Reproduced from data published in ref. 125.

Journal of Materials Chemistry A Accepted Manuscript

FIGURES:

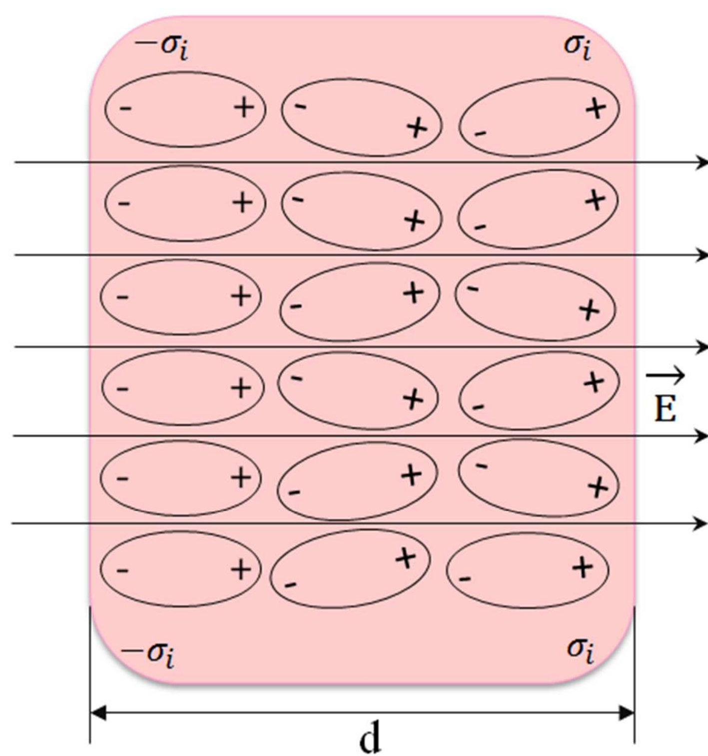

Figure 1

Journal of Materials Chemistry A Accepted Manuscript

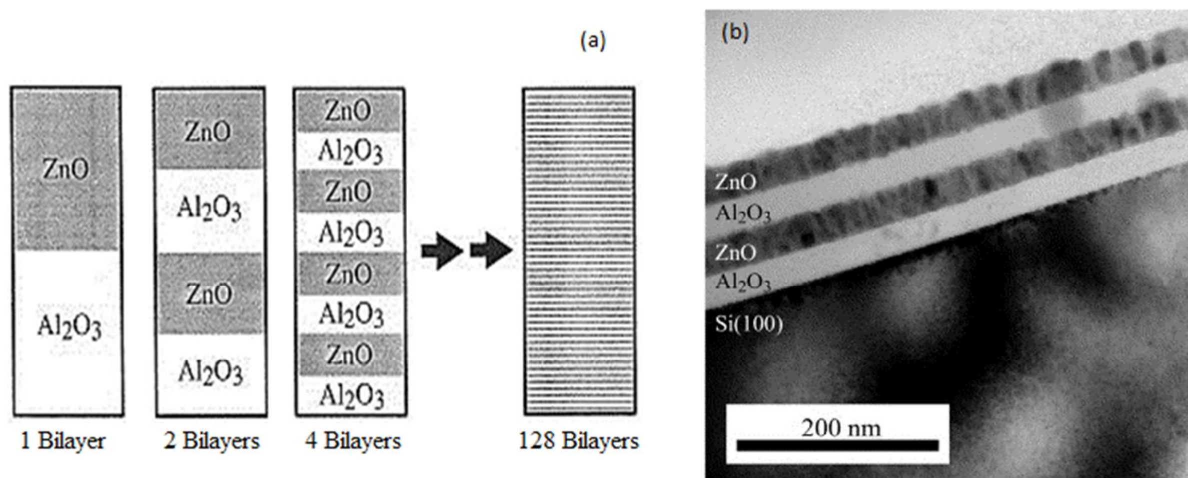

Figure 2

Journal of Materials Chemistry A Accepted Manuscript

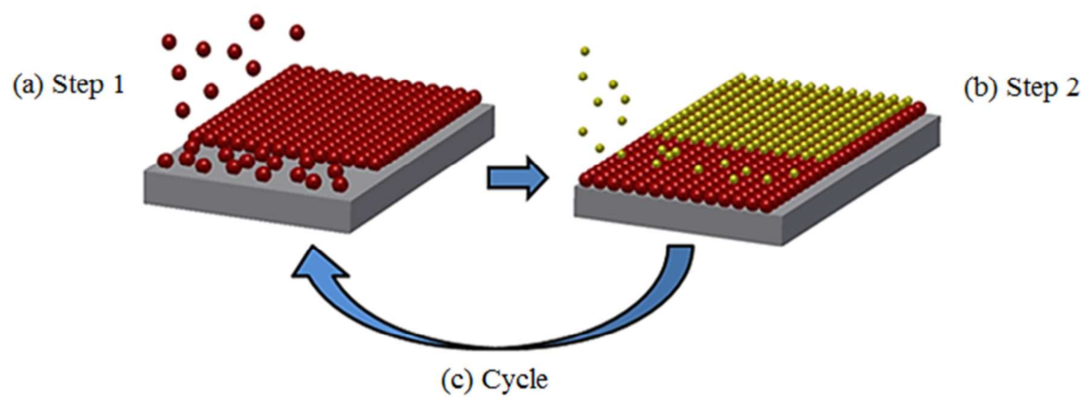

Figure 3

Journal of Materials Chemistry A Accepted Manuscript

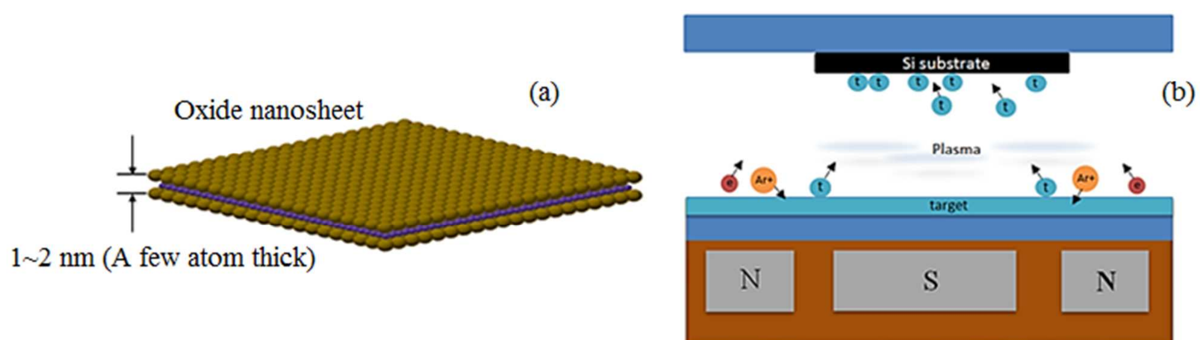

Figure 4

Journal of Materials Chemistry A Accepted Manuscript

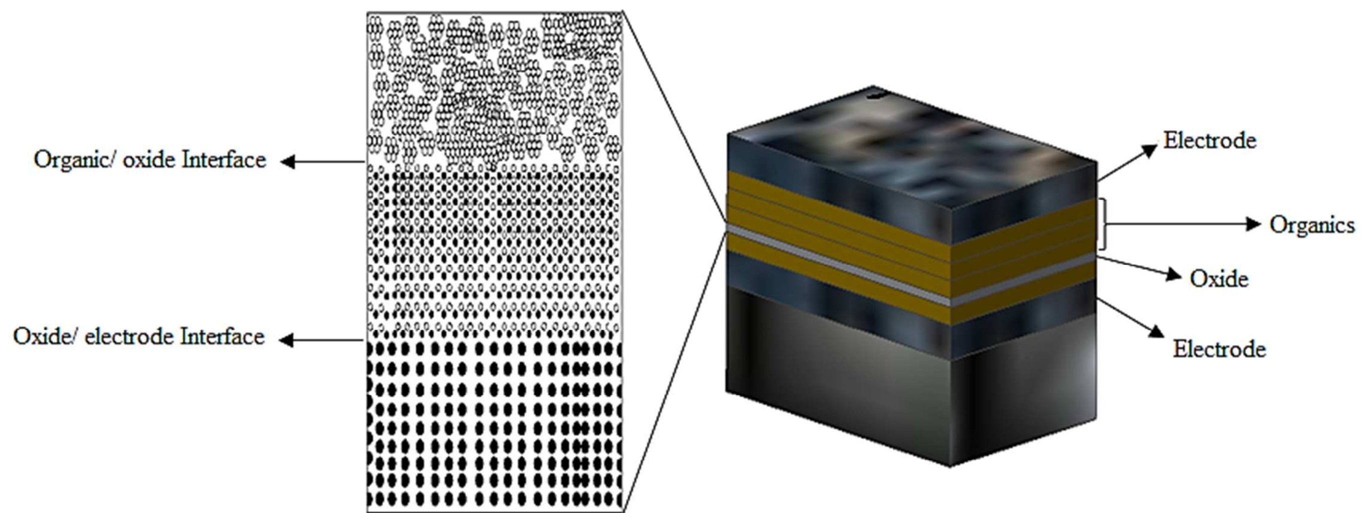

Figure 5

Journal of Materials Chemistry A Accepted Manuscript

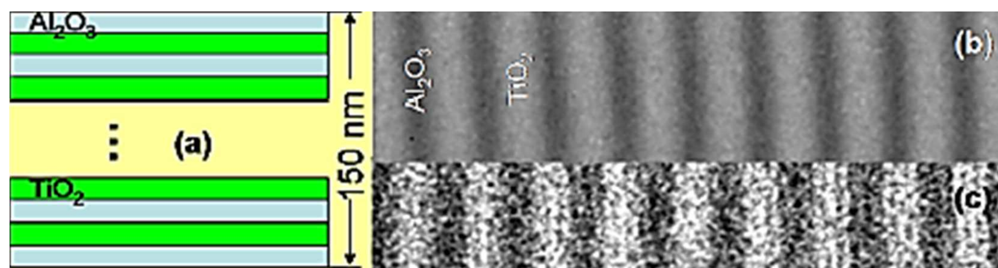

Figure 6

Journal of Materials Chemistry A Accepted Manuscript

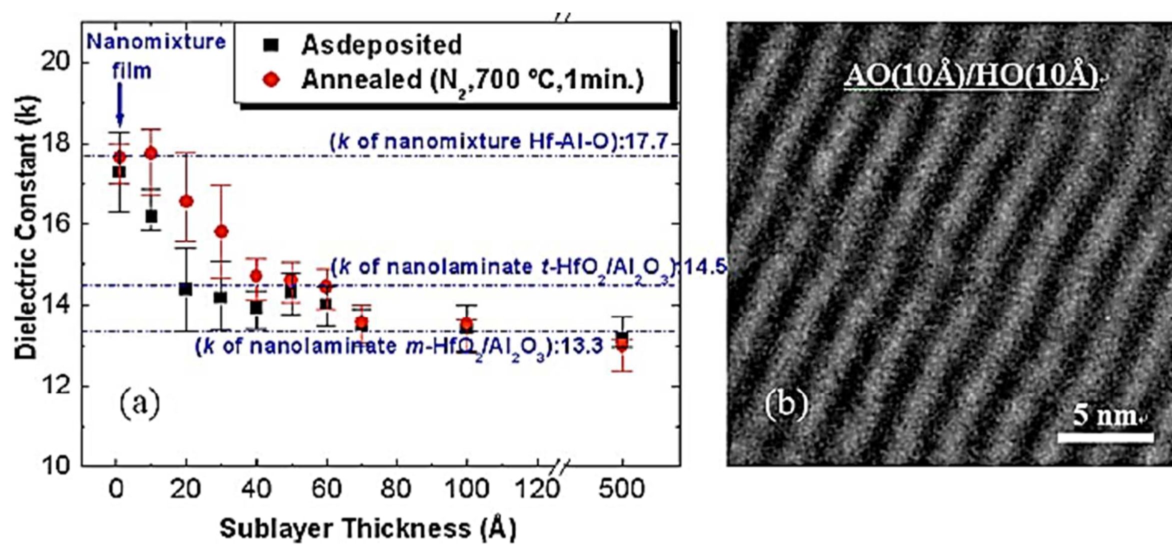

Figure 7

Journal of Materials Chemistry A Accepted Manuscript

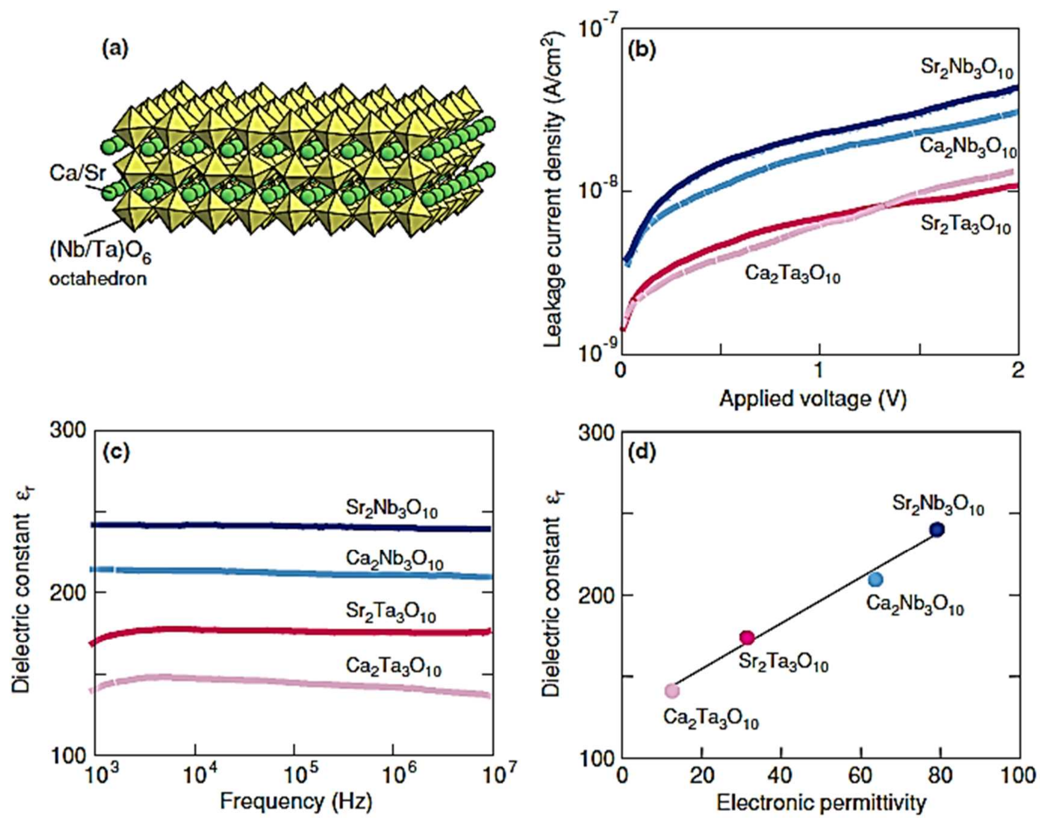

Figure 8

Journal of Materials Chemistry A Accepted Manuscript

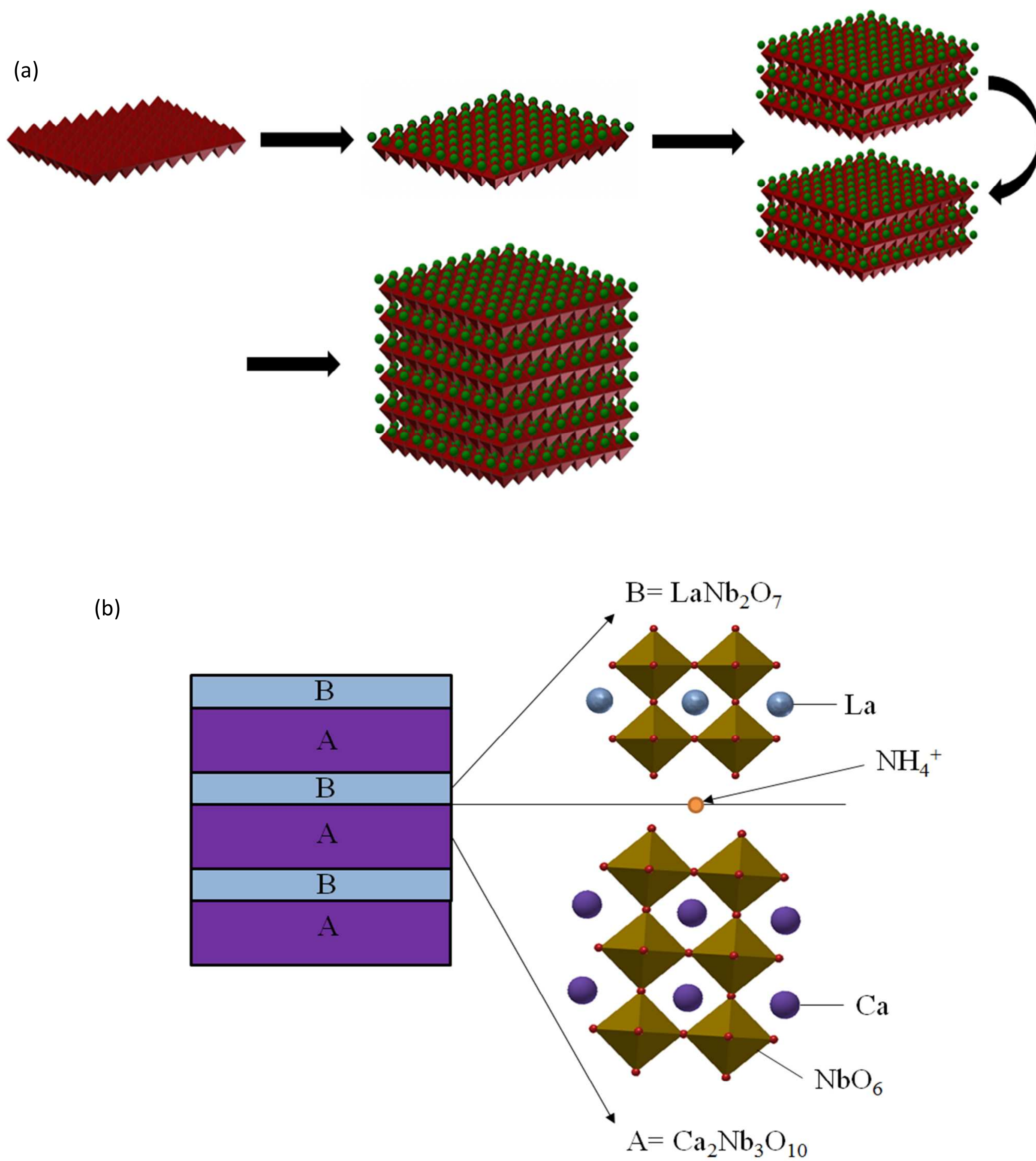

Figure 9

Journal of Materials Chemistry A Accepted Manuscript

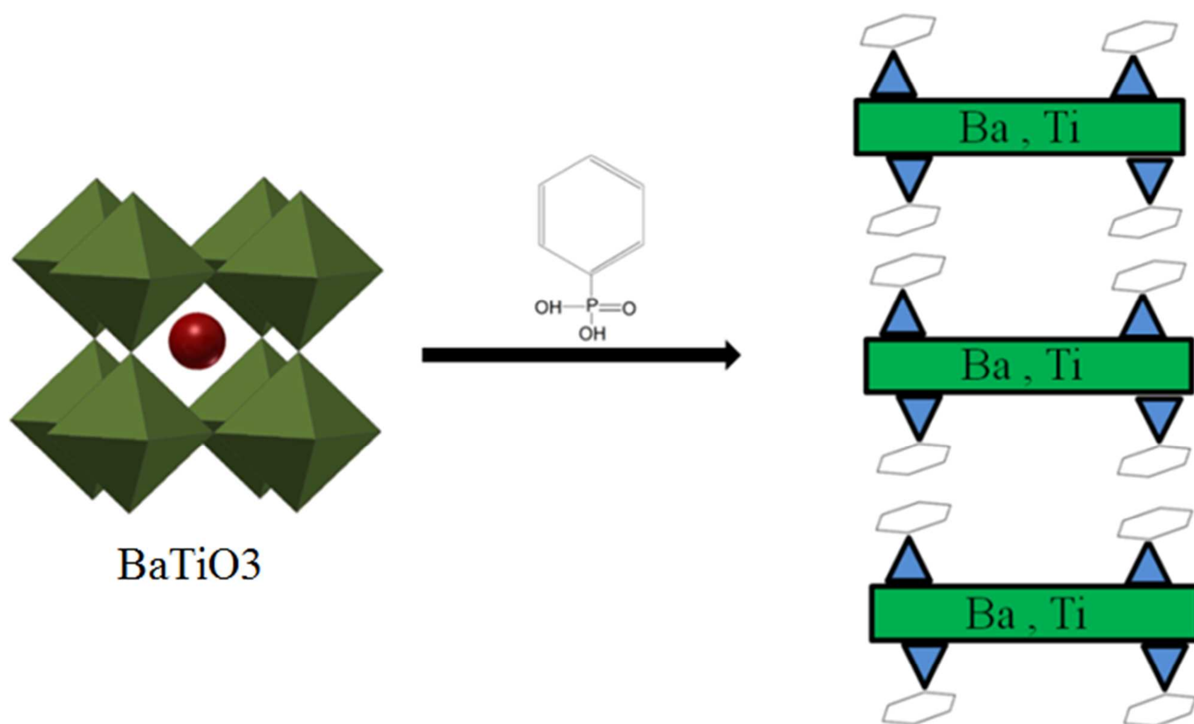

Figure 10

Journal of Materials Chemistry A Accepted Manuscript

TABLES:

Table 1. Dielectric constants (κ) of typical metal oxides and ferroelectric materials.

Composition	Dielectric Constant	Reference
SiO_2	3.9	[32]
Al_2O_3	9	[32]
ZrO_2	29	[32]
HfO_2	25	[32]
$HfSiO_4$	11	[1]
Ta_2O_5	26	[32]
La_2O_3	30	[32]
$LaAlO_3$	30	[1]
Nb_2O_5	35	[1]
TiO_2	95	[32]
$BaTiO_3$	1700	[1]
$SrTiO_3$	2000	[1]
$Pb(Zr,Ti)O_3$, $(Pb,La)(Zr,Ti)O_3$	2500	[33]
$CaCu_3Ti_4O_{12}$	80000	[1]

Journal of Materials Chemistry A Accepted Manuscript

Table 2. Highlights of selected nanolaminates systems.

Nanolaminate	Applications	Prominent characteristics	References
TiO_2/Al_2O_3	High dielectric application	Giant dielectric constant	[56]
Al_2O_3-TiO_2-Al_2O_3	High-κ gate dielectric	Low leakage	[93]
ZrO_2/Gd_2O_3	Capacitor Dielectrics	High dielectric constant high permittivity Thermal stability	[97]
ZrO_2/Al_2O_3	High-κ dielectric Gas diffusion barrier	Very promising as diffusion barrier	[27, 94, 104, 105]
Ta_2O_5/Al_2O_3	High-κ dielectric	Low κ Al_2O_3 dominates κ	[106, 107]
HfO_2/Al_2O_3	Great dielectric constant	Low leakage High dielectric constant	[87]
ZnO/Al_2O_3	Conductive oxide	Clear demonstration of substrate-inhabited nucleation effects.	[108]
Ta_2O_5/Nb_2O_5	High-κ gate dielectric	Reduced leakage over pure Ta_2O_5 at cost of some κ	[27]
Hf/Y/O	High-κ dielectric	Y_2O_3 deposition inhibited by HfO_2 deposition High Leakage	[109]
HfO_2/Ta_2O_5	High-κ dielectric	Reduce leakage over either pure film by orders of magnitude. Combines amorphous and crystalline as deposited films.	[110]
Zr-Al-Nb-O Alloy	High-κ gate dielectric	High dielectric constant. Low leakage.	[111]

Journal of Materials Chemistry A Accepted Manuscript

Table 3. Composition, synthesis and performance of some hybrid dielectrics. Reproduced from data published in ref. 120

Materials[a]	Methods[b]	T_s (□C)	C (nF/cm^2)	Structure	d (nm)[c]	J (A/cm^2)[d]	E_B (MV/cm)[e]
PVP/TiO_x	SC/sputter	175	-61	Bilayer	145–245	~10^{-5}	0.6
PVP/AlO_x	SC/sputter	175	31	Bilayer	145	~10^{-7}	4
PVP/YO_x	SC/evaporation	175	34–43	Bilayer	145–170	5×10^{-7}	2
PVP/YO_x	SC/evaporation	175	22–71	Bilayer	95–240	~10^{-7}	2
PVP/YO_x	SC/evaporation	175	33	Sandwich	140	1×10^{-7}	2
PMMA/AlO_x	SC/anodize	RT	11.4	Bilayer	220–260	n/r	n/r
PMMA/Ta_2O_5	SC/e-beam	RT	63.5	Bilayer	117	n/r	n/r
PVP/HfO_2	SC/ALD	200	8–15[f]	Sandwich	230–410	~10^{-8}	n/r
PVP/Al_2O_3	SC/ALD	152	~8	Sandwich	410–430	5×10^{-8}	n/r
PI/Ta_2O_5	MLD/ALD	170	45-94[f]	Nanolaminate	90–110	10^{-6} – 10^{-8}	n/r
pp-MCH/SiOCH	PECVD	RT	~9[f]	Nanolaminate	400	1×10^{-8} – 5×10^{-8}	n/r
Silicone/Al_2O_3	PECVD	105–120	20–45	Nanolaminate	65–225	5×10^{-9}	>5

[a]PVP = poly(4-vinylphenol); PMMA = poly(methyl methacrylate); PI = polyimide; pp-MCH = plasma polymerized-methylcyclohexane.
[b]SC = spin coating; ALD = atomic layer deposition; MLD = molecular layer deposition.
[c]d = total dielectric thickness.
[d]J = leakage current at an electric field E= 1 MV/cm.
[e]E_B = breakdown field defined by leakage current $J>10^{-6}$ A/cm^2.
[f]Estimate based on reported thickness and composition.

Journal of Materials Chemistry A Accepted Manuscript

Table 4. Dielectric constant of single and mixed metal phosphonates in polystyrene matrix. Reproduced from data published in ref. 125

Composition	Dielectric Constant
Pure Polystyrene (PS)	2.6±0.1
$BaTiO_3$/ 40 wt% PS	9.4±0.5
$SrTiO_3$/ 40 wt% PS	8.6±0.2
$BaTi(C_6H_5PO_3)_3$/ 40 wt% PS	19.4±0.2
$SrTi(C_6H_5PO_3)_3$/ 40 wt% PS	14.3±0.3
$Ba(C_6H_5PO_3)_3.H_2O$/ 40 wt% PS	4.6±0.1

Journal of Materials Chemistry A Accepted Manuscript